Front. Optoelectron. China 2010, 3(4): 364–369
DOI 10.1007/s12200-010-0124-7

RESEARCH ARTICLE

Mach-Zehnder interferometer based on core-cladding mode coupling in single mode fibers

Yan LIU[1], Bo LIU (✉)[1], Hao ZHANG[1], Yinping MIAO[2]

1 Key Laboratory of Opto-Electronic Information and Technology, Ministry of Education, Institute of Modern Optics, Nankai University, Tianjin 300071, China
2 Tianjin Key Laboratory of Film Electronic and Communication Devices, School of Electronics Information Engineering, Tianjin University of Technology, Tianjin 300384, China

Abstract In this paper, a novel simple but effective method is presented to construct compact all-fiber Mach-Zehnder (M-Z) interferometer based on CO_2-laser-machined micro-notches in single mode fibers. Interference fringes are obtained, and temperature, force, and bending characteristics of the interferometer have been experimentally investigated. Such a compact fiber component with acceptable sensing performances makes it a good candidate for the measurement of numerous physical parameters.

Keywords Mach-Zehnder (M-Z) interferometer, micro-notch, optical fiber sensor, single mode fiber

1 Introduction

Fabry-Pérot, Michelson, and Mach-Zehnder (M-Z) interferometers have been developed for sensing applications of various physical, chemical, and even biological measurands. These interferometers have several advantages such as high resolution and good electromagnetic immunity. The M-Z interferometer is particularly attractive owing to its simple configuration and highly sensitive interference fringes.

Fiber M-Z interferometer could be classified into two categories: extrinsic and intrinsic interferometers. The extrinsic M-Z interferometer is constructed by cascaded 3 dB couplers. The optical path difference varies when certain perturbation is applied on either of the two arms. Although extrinsic interferometers have found various applications, it is rather difficult to keep the two interference arms in the exact same environment. The intrinsic M-Z interferometer, however, has the sensor element built in the fiber itself and thus overcomes several problems that have to be resolved for extrinsic ones. By using a section of fiber with thermally expanded core [1], multimode fiber (MMF) [2], fiber-taper [3], laser-heating-induced micro-notches in photonic crystal fiber (PCF) [4], core-offset technique [4,5], PCF with collapsed micro-holes [6] or thin-core fiber (TCF) [7], one can construct an in-fiber M-Z interferometer where cladding modes are selectively excited and interfere with core mode when they partially couple back into the fiber core. However, some PCF-based M-Z interferometers have a high cost, and most of the others have relatively complex sensor structures.

In this paper, we propose a novel simple but compact method to achieve all-fiber M-Z interferometers. Two laser-machined micro-notches are introduced to a piece of conventional single-mode fiber to separate and recombine the light beam. Since the interferometer is constructed in the single-mode fiber with fairly simple structure, the proposed model is cost-effective and easy to fabricate. Its operating principle is analyzed in the next section and its spectral properties for some physical parameters will be presented later.

2 Device fabrication and operational principle

Figure 1 shows the schematic diagram of the proposed M-Z interferometer. To excite cladding modes, a micro-notch as a geometric perturbation is written in a single-mode fiber by CO_2 laser. The length of the micro-notch is about 10 μm, as estimated from the electron microscope image; and the notch depth is about 58 μm, just reaching the fiber core. Over the coupling region, the fiber without cladding

Received August 30, 2010; accepted September 19, 2010

E-mail: liubo@mail.nankai.edu.cn

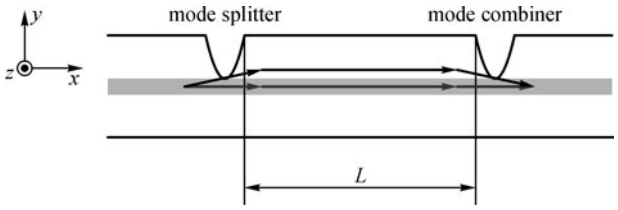

Fig. 1 Schematic diagram of proposed M-Z interferometer

is no longer a single mode fiber. Part of the fundamental core mode can be coupled to the cladding modes. If another micro-notch is written at a different position in the fiber, the coupled cladding modes may be re-coupled to the core mode again. Therefore, based on the cascaded configuration of two coupling regions, a very simple all-fiber Mach-Zehnder interferometer could be constructed. The segment between the coupling regions corresponds to the interference arms. Suppose only one cladding mode is excited, then the optical length difference results from two parts: coupling region component and propagating region component. Although the former is decided by both propagation distance and refractive indices, it remains constant when L changes. The optical path difference for this region is described as Δ_1. While for the propagating region, the physical lengths are exactly the same but the optical path difference still exists due to the different effective refractive indices [4], and thus the total phase difference between the core mode and the mth order cladding mode is

$$\delta = \frac{2\pi}{\lambda}[\Delta_1 + (n_{co} - n_{cl,m})L], \quad (1)$$

where n_{co} and $n_{cl,m}$ are the effective refractive indices of core mode and the mth order cladding mode, respectively. λ refers to wavelength and L is the distance between the two coupling regions. Let I_{co} and I_{cl} represent optical intensities of the core mode and cladding mode, respectively, the total output optical intensity could be expressed as [8]

$$I = I_{co} + I_{cl} + 2\sqrt{I_{co}I_{cl}}\cos\left\{\frac{2\pi}{\lambda}[\Delta_1 + (n_{co} - n_{cl,m})L]\right\}. \quad (2)$$

From Eqs. (1) and (2), it is easy to find that the change of the effective refractive indices or length L will result in the variation of optical path difference. Therefore, it is possible to achieve the measurement of physical or chemical parameters by monitoring the variation of interference fringes.

Transmission spectra of the proposed interferometer are measured for different interference arm lengths, as shown in Fig. 2. Interference fringes with a high visibility are observed throughout a wavelength range of 600–1700 nm and the fringes do not possess uniform wavelength spacing. For clarity, only the region between 1150–1650 nm is illustrated in the figure. It should be noted that the wavelength spacing becomes smaller when the interferometer length L increases. It is easy to understand the reason for this phenomenon according to Eq. (2). n_{co} and $n_{cl,m}$ are constants for certain modes, and thus, $2\pi(n_{co} - n_{cl}^{i})L$ is also invariable. However, the fringe spacing is unequal as wavelength is the denominator in Eq. (2). Moreover, the phase difference becomes larger due to the increase in L, resulting in narrower wavelength spacing in the interference fringes. In addition, besides the first order cladding mode, many higher order mode coupling may be excited as well, which makes the interference fringes much more complex.

To fabricate the proposed modal interferometer, only a section of single-mode fiber is required. The fiber is placed around the focus of a CO_2 laser to achieve effective laser illumination. The distance L between the micro-notches can be controlled via the scanning CO_2 laser. Two coupling regions are fabricated at the same time to ensure the same physical conditions for the two micro-notches. A super continuum light source and an optical spectrum analyzer (OSA) with a resolution of 0.1 nm were employed to monitor the transmission spectra in real time. Obviously, the CO_2 laser induces the fiber ablation on the illumination side, and large deformation turns up close to the fiber core, as shown in Fig. 1.

3 Experimental investigation of characteristics to some physical parameters

Temperature, force, and bending characteristics of the proposed M-Z interferometer are experimentally investigated. The arm length of the M-Z interferometer for our study is 2 cm. The insertion loss almost depends on the quality of fiber splicing and if fiber is fused in a proper way, the insertion loss could be controled within 1 dB.

3.1 Temperature characteristics

Figure 3 shows the temperature response at peak wavelength of our interferometer from 30°C to 90°C. It can be seen that the interference peak shifts toward longer wavelength as temperature increases. The temperature sensing principle could be attributed to the interference between the core mode and cladding modes in single mode fibers, like the long period fiber grating (LPFG)-based temperature sensor, which employs the thermo-optic coefficient difference of the core mode and cladding mode refractive indices.

3.2 Force characteristics

To investigate the force characteristics of the interference fringes, three types of force are applied on the interferometer, including lateral plane force, lateral point force

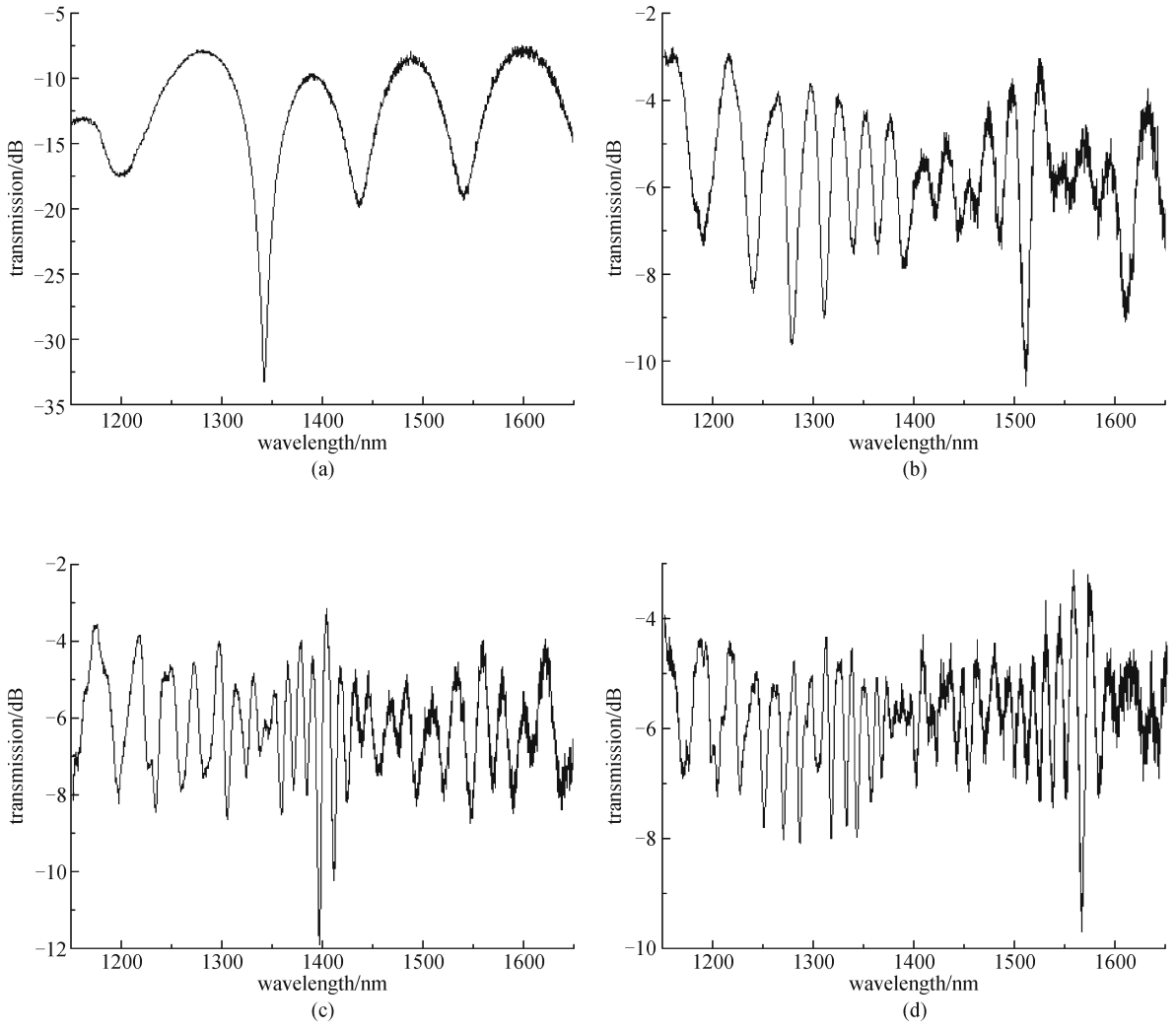

Fig. 2 Measured wavelength spectra for different interference arm lengths. (a) $L = 5$ mm; (b) $L = 20$ mm; (c) $L = 30$ mm; (d) $L = 40$ mm

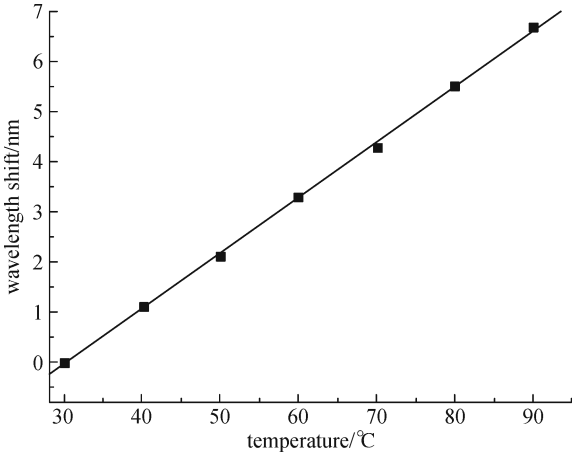

Fig. 3 Peak wavelength shift as a function of temperature

and axial force. However, none of them exhibits distinguishable fringe variation including change of transmission loss and peak wavelength shift, as shown in Fig. 4. The fluctuation of transmission loss has no orderliness with a maximum value of no more than 0.5 dB, which may be attributed to instability of the light source power. Therefore, the applied force does not have a distinguishable impact on transmission loss within the measured force range. The case for larger force range was not investigated in our experiment considering the fragility endurance of the test fiber.

The above phenomena can be explained as follows. First, in order to protect the fiber, different kinds of force not large enough to cause considerable transmission loss are applied. Second, the phase difference change $\Delta\delta$ induced by an elongation and photoelastic effect can be approximately given by [9]

$$\Delta\delta = \frac{2\pi}{\lambda}[\Delta n \Delta L + \Delta(\Delta n)L], \tag{3}$$

where $\Delta n = n_{\mathrm{co}} - n_{\mathrm{cl},m}$, and $\Delta(\Delta n) = \Delta n_{\mathrm{co}} - \Delta n_{\mathrm{cl},m}$.

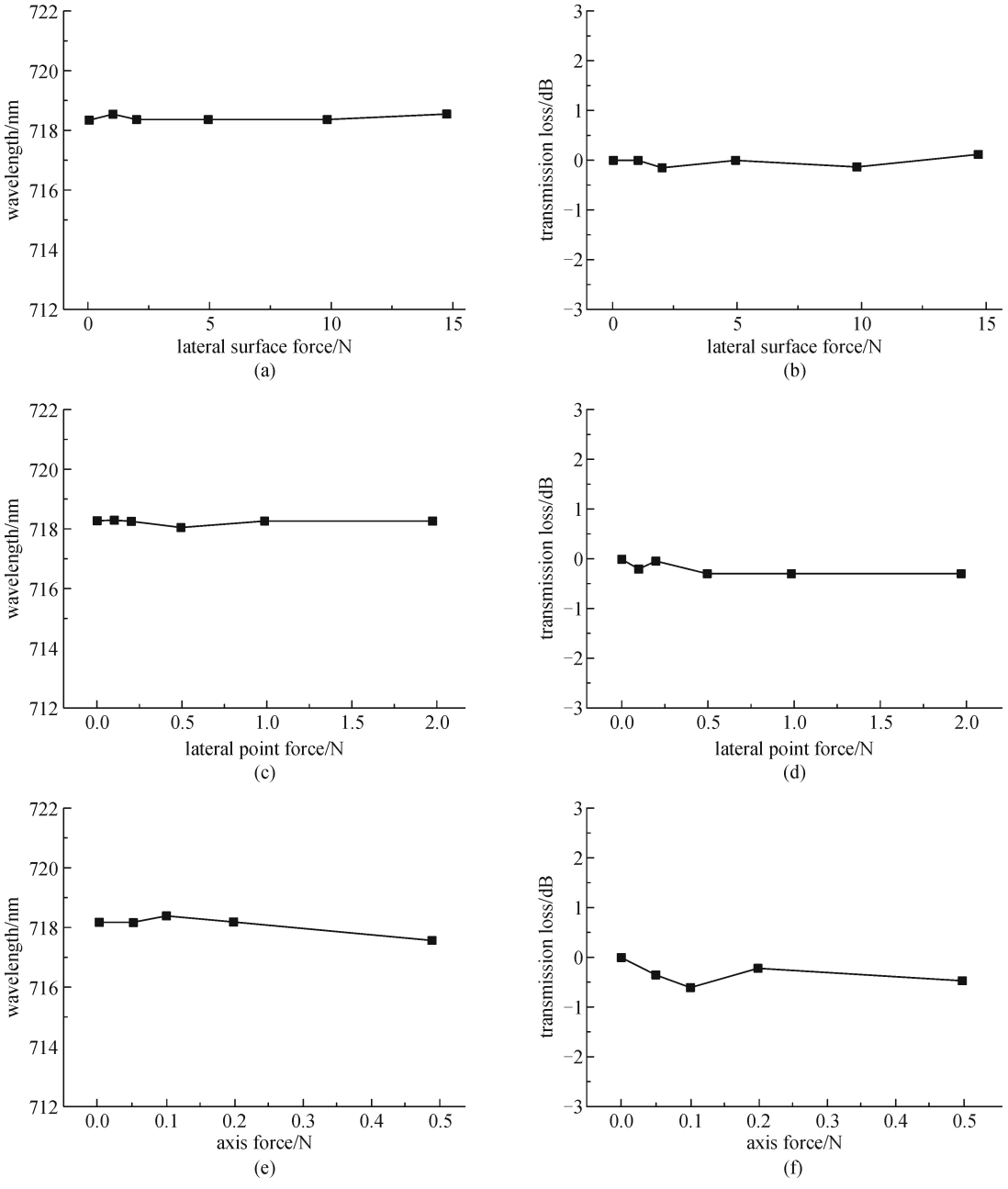

Fig. 4 Force characteristics in three different cases. (a) and (b) for lateral plane force; (c) and (d) for lateral point force; (e) and (f) for axial force (A peak around 718 nm is studied)

As for lateral force, the force hardly induces any axial length elongation ΔL. In addition, taking axial force into consideration, no more than 0.5 N force is applied, leading to only about 10 μm axial length elongation ΔL, far less than the 2 cm interference arm length, and thus producing a negligible longitudinal strain ($\Delta L/L \approx 0$). Therefore, the phase difference change $\Delta\delta$ in Eq. (3) is only determined by $\Delta(\Delta n)$ for a specific wavelength. The birefringence variation Δn per unit length of the core refractive index under the lateral force could be expressed as [10]

$$\Delta n = \frac{4kF}{\pi rLE}, \tag{4}$$

where k is the strain optical coefficient, F is the applied force, r and E are the outer radius and Young's Modulus of the fiber, respectively. When the force is applied, the two interference modes approximately experience the same amount of variation according to Eq. (4). Thus the difference between effective refractive index changes of the two modes is almost zero and the phase difference

remains constant. In this condition, the transmission spectrum will not vary with the change in applied force.

The transmission spectra are not affected by the lateral plane force, lateral point force and axial force within a certain range, which makes it possible to construct force-independent sensors.

3.3 Bending characteristics

Bending characteristics of the proposed M-Z interferometer are orientation-dependent due to its asymmetry. Figure 5 shows the transmission spectra of a peak around 702.4 nm with the bending curvature radius between infinity and 6 cm along two orthogonal directions. When the fiber bends in the *x*-*y* plane, making the coupling points on the outer circle, both the peak wavelength and transmission loss vary. The peak wavelength exhibits a slight blue-shift from 702.8 to 701.9 nm and the transmission loss increases from about −7.43 to −8.38 dBm as the radius decreases. However, when bending takes place in the *x*-*z* plane, only transmission loss changes from about −4.67 to −6.42 dBm while the peak wavelength does not shift.

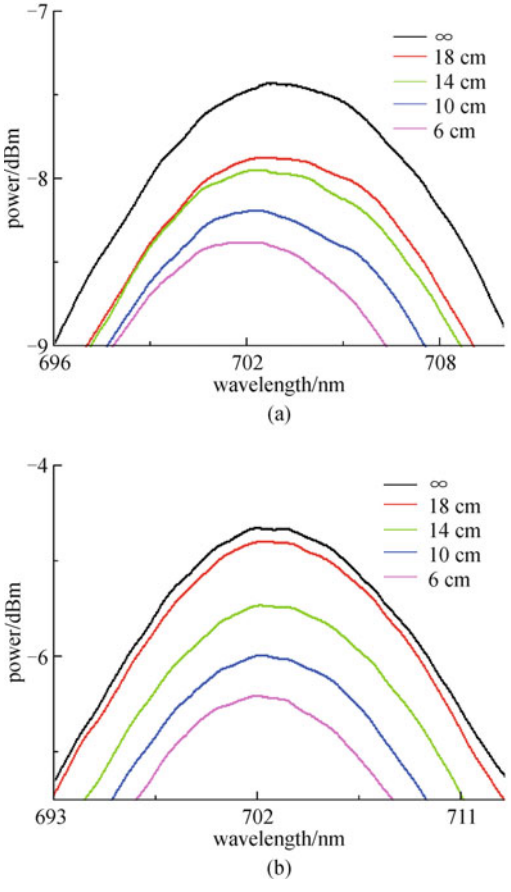

Fig. 5 Spectra responds with bending radius decreases. (a) Bending in *x*-*y* plane; (b) bending in *x*-*z* plane

When bending is applied, some modes do not comply with the total reflection condition any longer, and hence leak off the fiber. Besides, at the coupling point, the number of excited cladding modes and the coupling energy decreases, this also results in lager transmission loss. In addition, if bending occurs in the *x*-*y* plane and the coupling points are located around the outer circle, the physical path of cladding modes is quite enlarged because of the fiber elongation, while since the core mode is located in the neutral layer and its physical path does not change, which leads to the decrease of phase difference, and consequently the peak wavelength accordingly moves towards the shorter wavelength direction. However, if bending occurs in the *x*-*z* plane, the optical paths of core mode and cladding mode are both in the neutral layer, and hence bending has no effect on phase difference and peak wavelength shift.

4 Conclusion

We have demonstrated a simple but effective method to implement compact in-line all-fiber Mach-Zehnder interferometers based on CO_2-laser-machined micro-notches. Interference fringes were experimentally obtained. Experimental results indicate that the proposed interferometer has acceptable temperature and bending sensitivities, and these measurements are not affected by lateral plane force, lateral point force and axial force within a certain range.

The proposed M-Z interferometer based on micro-notches configuration has several advantages such as simple structure, high stability, low cost, and compact size.

Acknowledgements This work was jointly supported by the National Key Natural Science Foundation of China (Grant No. 60736039), the National Natural Science Foundation of China (Grant Nos. 10904075, 11004110, 50802044), the Fundamental Research Funds for the Central Universities, the National Key Basic Research and Development Program of China (No. 2010CB327605).

References

1. Nguyen L V, Hwang D, Moon D S, Chung Y. Tunable comb-filter using thermally expanded core fiber and ytterbium doped fiber and its application to multi-wavelength fiber laser. Optics Communications, 2008, 281(23): 5793–5796
2. Nguyen L V, Hwang D, Moon S, Moon D S, Chung Y. High temperature fiber sensor with high sensitivity based on core diameter mismatch. Optics Express, 2008, 16(15): 11369–11375
3. Lu P, Men L, Sooley K, Chen Q. Tapered fiber Mach-Zehnder interferometer for simultaneous measurement of refractive index and temperature. Applied Physics Letters, 2009, 94(13): 131110
4. Choi H Y, Kim M J, Lee B H. All-fiber Mach-Zehnder type interferometers formed in photonic crystal fiber. Optics Express,

2007, 15(9): 5711–5720

5. Tian Z, Yam S S H, Loock H P. Single-mode fiber refractive index sensor based on core-offset attenuators. IEEE Photonics Technology Letters, 2008, 20(16): 1387–1389
6. Villatoro J, Finazzi V, Badenes G, Pruneri V. Highly sensitive sensors based on photonic crystal fiber modal interferometers. Journal of Sensors, 2009, 2009(2009): 747803
7. Xia T H, Zhang A P, Gu B, Zhu J J. Fiber-optic refractive-index sensors based on transmissive and reflective thin-core fiber modal interferometers. Optics Communications, 2010, 283(10): 2136–2139
8. Lee B H, Nishii J. Dependence of fringe spacing on the grating separation in a long-period fiber grating pair. Applied Optics, 1999, 38(16): 3450–3459
9. Dong X Y, Yang X F, Shum P, Chan C C. Tunable WDM filter with 0.8-nm channel spacing using a pair of long-period fiber gratings. IEEE Photonics Technology Letters, 2005, 17(4): 795–797
10. Rashleigh S. Origins and control of polarization effects in single-mode fibers. Journal of Lightwave Technology, 1983, 1(2): 312–331